



ENERGISATION METHOD FOR OFFSHORE WIND FARMS CONNECTED TO HVDC VIA DIODE RECTIFIERS

Oscar Saborío-Romano¹, Ali Bidadfar², Jayachandra N. Sakamuri³, Nicolaos A. Cutululis¹

¹ – Technical University of Denmark, Denmark
osro@dtu.dk

² – Ørsted Offshore, Denmark

³ – Vattenfall, Denmark

Abstract – Diode rectifiers (DRs) have been recently suggested as a viable alternative for connecting offshore wind farms (OWFs) to HVdc, eliciting growing interest from both industry and academia. However, energisation of DR-connected OWFs is not straightforward. The present study constitutes a proof of concept of a novel energisation method for DR-connected OWFs, in which auxiliary power is provided from the shore through the HVdc link and the dc bus bar of one or more WTs. The proposed method provides an alternative with minimal additional hardware, which can be easily extended to more WTs in the OWF, increasing reliability by providing redundancy. The study includes coinciding auxiliary loads with active and reactive power components and a semi-aggregated OWF model, in which every WT is individually represented in the string containing the energising WT. An additional sequence of simulation events is considered following the initial energisation sequence. Such sequence comprises wind power taking over the provision of the auxiliary power. The simulation results indicate that the proposed method is a suitable alternative for energising OWFs connected to HVdc via DRs.

Keywords: Diode-rectifier-based HVdc transmission – Energisation – Grid-forming wind turbine control – Off-shore wind energy integration



1 INTRODUCTION

Electrical infrastructure connecting offshore wind farms (OWFs) to the onshore networks is required to exploit Europe's offshore wind resources further. Thus far, only a few OWFs are connected through HVdc, while the majority export their production via HVac. However, the amount of HVdc-connected OWFs is widely expected to increase, as the associated costs decrease and the distance from shore and size of new OWFs increase [1].

HVdc transmission technology employing voltage source (forced-/self-commutated) converters (VSCs), based on insulated- gate bipolar transistors, has developed significantly since its introduction in 1997. Such technology provides advantages like smaller footprints, fast reversibility of active power flow, independent control of active and reactive power, and the (grid-forming) capability to form ac networks, i.e. to control their ac-side voltage magnitude and frequency. Due to such advantages, the use of VSC-based offshore HVdc terminals has made it possible to develop HVdc-connected OWFs with the prevailing grid-following approach to the control of wind turbines (WTs), in which WTs rely on other (grid-forming) units (e.g. VSC-based offshore HVdc terminals) forming their ac network.

In quest of lowering costs further, (uncontrolled, line-commutated) diode rectifiers (DRs) have been recently suggested as a viable alternative for connecting OWFs to HVdc, eliciting growing interest from both industry and academia [2]–[16]. DR-based offshore HVdc terminals may provide advantages such as even smaller footprints, higher reliability, lower costs and higher efficiency [5], [8]. However, such offshore HVdc terminals lack the grid-forming capability of VSCs, for diodes are passive devices. WTs have consequently been proposed as viable candidates to take over such responsibility, which requires changing their control approach from that of grid-following units to that of grid-forming units [2], [7].

1.1. WIND FARM ENERGISATION

WTs and WFs have auxiliary systems (i.e. loads) that need electricity most of the time. Such loads can consist of pitch and yaw motors, navigation lights, oil pumps, air conditioning, dehumidifiers, and measurement, control, protection, communication and safety systems, among others.

When WTs produce electricity, part of the production is used to supply such loads, but auxiliary power must be otherwise provided from local auxiliary energy sources, e.g. batteries or diesel generators, or from the networks connected to them [1]. This is the case when there is no aerodynamic power available from the wind (i.e. the wind speed is below the cut-in wind speed or above the cut-out wind speed of the WTs) or before WTs are ready to produce power.

The use of VSC-based offshore HVdc terminals allows remote OWFs to draw the auxiliary power required in such cases from the HVdc networks connected to them. This, however, is not possible for OWFs connected to HVdc via DRs, as power through the DRs can only flow towards the shore. As a consequence, such OWFs must be energised by other means. This is also the case for OWFs connected to HVdc networks via VSCs, when such offshore converters are not operational [1], [17]–[19].

Different solutions have been proposed for energising OWFs connected to HVdc via DRs [4], [6], [9]. The use of local auxiliary energy sources or the connection to neighbouring energised offshore ac networks, e.g. other OWFs, have been proposed in [6]. The latter has been considered in several subsequent studies [11].

Solutions for providing the auxiliary power from onshore ac networks are represented in grey in Figure 1. Some of these rely on additional long submarine cables connecting the onshore ac networks and the OWFs. The use of additional LVdc links has been proposed in [6], which requires additional VSC-based power conversion terminals. Moreover, additional MVac *umbilical* cables interconnecting the onshore and offshore ac networks have been introduced in [6]–[9]. Such umbilical cables have been considered in several subsequent studies [10]–[14], [16], and have been assumed to be disconnected during normal operation, i.e. their use has been restricted to the energisation of the corresponding OWFs. Other solutions avoid the need for additional long submarine cables by introducing additional power conversion equipment offshore to effectively bypass the DRs during energisation [4], [6].

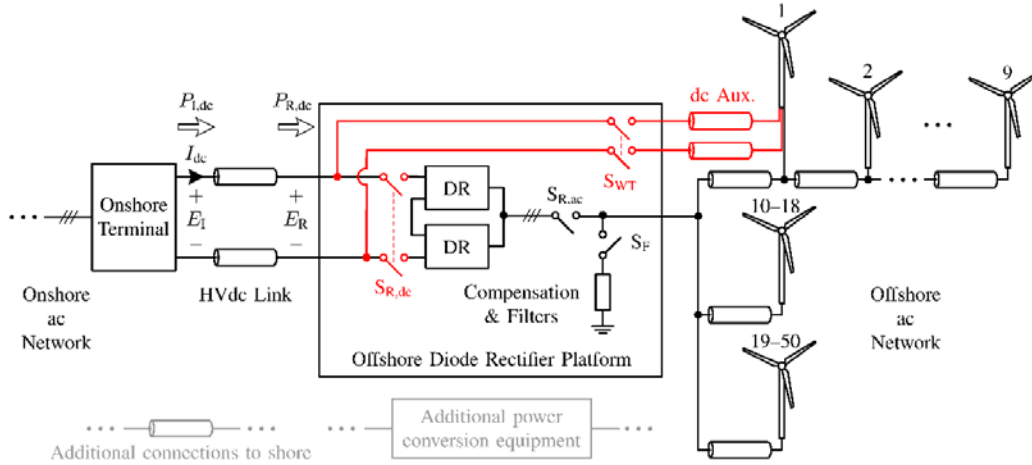


Figure 1: Overview of the studied system; additional equipment introduced by the proposed energisation method is highlighted in red; alternatives in literature for providing the auxiliary power from onshore ac networks are highlighted in grey

In pursuit of increasing reliability and lowering costs and environmental impact, a new energisation method has been proposed in [20] for the case of an OWF connected to an onshore ac network through an HVdc link having a DR-based offshore terminal and a full-bridge-VSC-based onshore terminal. During energisation, auxiliary power is provided from the shore through the HVdc link and the dc bus bar of one or more WTs. The method only requires short additional dc cables connecting the dc bus bar of such *energising* WT to the HVdc link, and corresponding dc disconnectors at the cable terminals and at the dc terminals of the DR platform, highlighted in red in Figures 1 and 2.

This work extends the assessment in [20] to include coinciding auxiliary loads with active and reactive power components and a semi-aggregated OWF model, in which every WT in the string containing the energising WT is represented individually. An additional sequence of simulation events is considered following the initial sequence, in which the OWF is energised with the proposed method. In the second sequence, wind power takes over the provision of auxiliary power, once enough aerodynamic power becomes available from the wind and WTs are ready to produce power.

The rest of the paper is organised as follows. The studied system and the main control algorithms are described in Section 2. In Section 3, the considered sequences of events are described, and corresponding simulation results are presented and discussed. Finally, concluding remarks are made in Section 4.

2 MODELLING AND CONTROL

Figure 1 shows an overview of the studied system. The system is based on that described in [11], [12] and consists of one of three 400 MW OWFs connected to an onshore ac network by means of a 200 km long 1200 MW ± 320 kV monopolar HVdc link and corresponding onshore HVdc terminal, operating at a third of the rated voltage (i.e. the nominal voltage is approximately 213 kV, and the nominal power is 400 MW). Balanced/symmetric operation is assumed. The offshore HVdc terminal: one of three diode rectifier platforms (one per OWF), depicted in Figure 1, consists of two (uncontrolled, line-commutated) diode-based 12-pulse rectifiers (DRs) connected in series, with corresponding reactive power compensation and filter bank on their ac side.

The OWF has 50 type-4 (full-converter) 8 MW WTs, laid out in 6 strings. The WT converter nominal ac voltage is 3.3 kV. WTs 1–9 in the first string are represented individually. WTs 10–18 in the second string, are aggregated into an equivalent 72 MW WT and corresponding cable equivalent π circuit. Likewise, WTs 19–50 in the other 4 strings are aggregated into an equivalent 256 MW WT and corresponding cable equivalent π circuit.

The front-end (line-side) network of the k th wind turbine(s), WT_k , is shown in Figure 2. The coinciding auxiliary loads are represented within each (equivalent) WT by a constant power load, with an active power component, $P_{a,k}$, corresponding to 0.2 % of the nominal power (800 kW in total for the whole 400 MW WF) and a power factor of 0.83, i.e. a reactive power component, $Q_{a,k}$, corresponding to 0.134 % of the nominal power (536 kVar in total for the whole 400 MW WF).

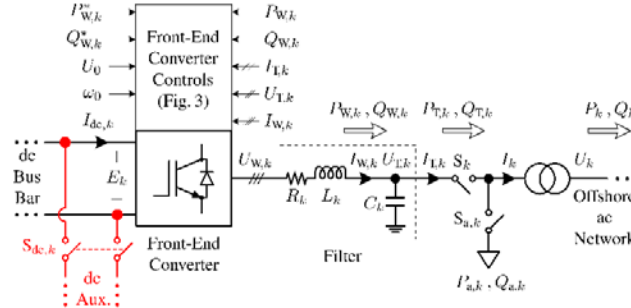


Figure 2: Front-end (line-side) network of the k th wind turbine(s); additional equipment introduced in the energising wind turbine(s) by the proposed energisation method are highlighted in red

WT₁ is chosen as the energising WT: its dc auxiliary supply terminal can be connected to that of the DR platform by means of additional dc auxiliary cables. Additional dc disconnectors are also introduced at the corresponding terminals, $S_{dc,1}$, S_{WT} , and at the dc terminals of the DR platform, $S_{R,dc}$. The additional equipment introduced by the method is shown in Figures 1 and 2, highlighted in red. The HVdc link dynamics are assumed to dominate in the energisation path. The influence of the other elements, e.g. dc auxiliary cables, effectively interconnecting the HVdc link and the dc bus bar of WT₁ (when S_{WT} is closed) is thus neglected, i.e. the voltage at the dc bus bar of WT₁, E_1 , is approximately equal to the voltage at the offshore terminal of the HVdc link, E_R , during energisation.

WT rotor and back-end (generator-side) network dynamics are not considered, as they are not relevant to the case in question. Pulse-width modulation (PWM) is assumed to be done in the linear range, switching effects and any delay due to the implementation of the PWM are neglected, and average value models are used to represent the WT FECs. Focus is given to dynamics not faster than the WT FEC (inner/lower) current control loops, which are designed to have a bandwidth of 200 Hz.

2.1. WIND TURBINE FRONT-END CONVERTER CONTROLS

The grid-forming WT FEC controls, shown in Figure 3, are based on those proposed in [15] and are implemented on a rotating reference frame (RRF) with angular speed given by ω_k , oriented on the voltage at the filter capacitor, $U_{T,k}$, and with the quadrature (q) axis leading the direct (d) axis by 90° .

In each WT front-end network, the filter capacitor voltage direct (d) and quadrature (q) axis components are regulated by the FEC lower/inner control loops to follow the corresponding references, $U_{Td,k}^*$, $U_{Tq,k}^*$, respectively. $U_{Td,k}^*$ consists of two components: the offshore ac network voltage set point, U_0 , common to all WTs, and a component individual to each WT, which is altered to control the FEC active power output, $P_{W,k}$. In an additional control loop based on the FEC phase-locked loop (PLL), a proportional regulator manipulates $U_{Tq,k}^*$ to control ω_k . The reference to such additional loop also consists of two components: the offshore ac network (angular) frequency set point, ω_0 , common to all WTs, and a component individual to each WT, which is altered to control the FEC reactive power output, $Q_{W,k}$. When the WF is exporting power, the FEC upper/outer control loops in each WT regulate $P_{W,k}$ and $Q_{W,k}$ as follows. A proportional-integral (PI) regulator controls $P_{W,k}$ to follow the corresponding reference, $P_{W,k}^*$, whereas $Q_{W,k}$ is controlled by a proportional regulator (reactive-power-frequency droop) with a given reference, $Q_{W,k}^*$, so that reactive power is shared among WT FECs (avoiding overcurrents and reactive current circulation).

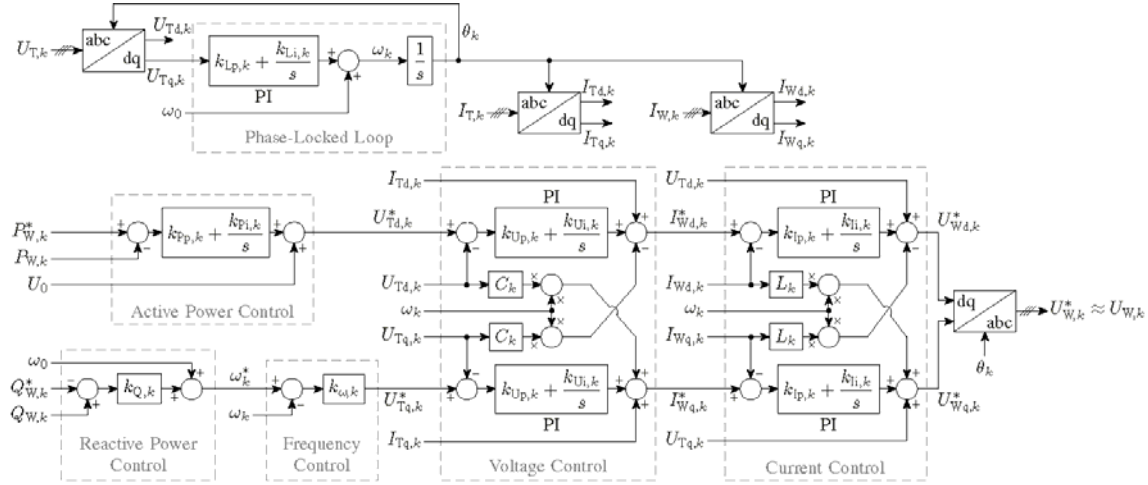


Figure 3: Front-end (line-side) converter controls of the k th wind turbine(s)

3 SIMULATION RESULTS

Results of the dynamic simulations performed in PSCAD are shown in Figure 4. All (equivalent) WT front-end networks and corresponding converter controls have the same parameter per-unit (pu) values. Moreover, $\omega_0 = 1$ pu for all of them. Quantities related to the HVdc link are depicted in (a)–(c). The voltage at the onshore and offshore ends of the HVdc link, E_l and E_R , respectively, are illustrated in (a), while the HVdc link current, I_{dc} , is portrayed in (b). Likewise, the active power flowing out of the onshore terminal, $P_{l,dc}$, and into the offshore diode rectifier platform, $P_{R,dc}$, are illustrated in (c).

The remaining (d)–(h) depict quantities related to the offshore ac network. The offshore ac network (angular) frequency, ω , is portrayed in (d), whereas the WT terminal rms voltages, U_k , and output rms currents, I_k , are presented in (e) and (f), respectively. Finally, the WT active and reactive power output, P_k and Q_k , respectively, are shown in (g) and (h), respectively.

Table 1 summarises the simulation events, which are discussed in the following. The events are grouped in sequences to facilitate discussion. Two consecutive sequences of events have been considered. Sequence 1, depicted on the left of Figure 4, corresponds to the energisation of the OWF with the proposed method. In Sequence 2, portrayed on the right of Figure 4, wind power takes over the provision of the auxiliary power, once enough aerodynamic power becomes available from the wind and WTs are ready to produce power.

Initially, the aerodynamic power available from the wind is assumed to be 0, i.e. the wind speed is assumed to be below the cut-in wind speed or above the cut-out wind speed of the WTs. The WTs, offshore ac network and HVdc link are de-energised, the voltage and WT active/reactive power set points, E_R^* , U_0 , $P_{W,k}^*$, $Q_{W,k}^*$, are set to 0, and all ac circuit breakers and dc disconnectors, shown in Figures 1 and 2, are open. The regulators in the WT FEC PLL and frequency and active/reactive power controls are disabled for all WTs. In this way, $\omega_k = \omega_0$, $U_{Td}^* = U_0$, $U_{Tq}^* = 0$ and the WT FEC controls are equivalent to those used in [20].

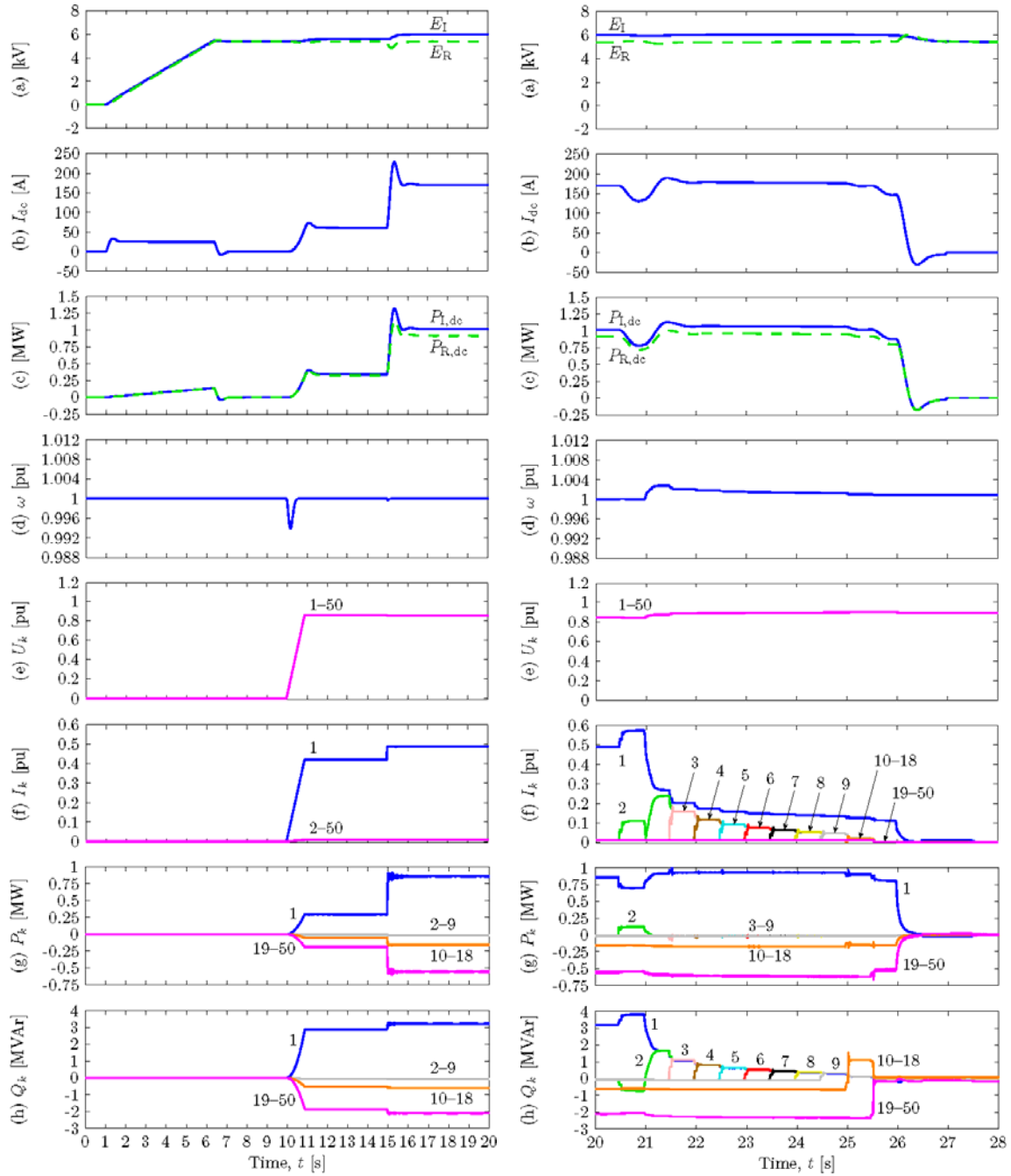


Figure 4: Simulation results for Sequence 1 (left) and Sequence 2 (right); (a) voltage at the onshore and offshore ends of the HVdc link, E_I and E_R , respectively; (b) HVdc link current; (c) active power flowing out of the onshore terminal, $P_{I,dc}$, and into the offshore diode rectifier platform $P_{R,dc}$; (d) offshore ac network (angular) frequency; (e) WT_k terminal rms voltage; (f) WT_k output rms current; (g) WT_k active power output; (h) WT_k reactive power output; values of k indicated next to each visible trace within each plot



Table 1: Simulation events

Time [s]	Events
< 0	No power available from the wind; WTs, offshore ac network and HVdc link de-energised; E_R^* , U_0 , $P_{W,k}^*$ and $Q_{W,k}^*$ set to 0; all ac circuit breakers and dc disconnectors open; FEC PLL and frequency and (active/reactive) power controls disabled for all WTs
Sequence 1: Energisation from Shore	
0	S_{WT} and $S_{dc,1}$ closed: dc auxiliary supply effectively connects the dc bus bar of WT ₁ to the HVdc link
1 – 6.39	E_R^* increased from 0 to 5.39 kV; onshore terminal energises the HVdc link and the dc bus bar of WT ₁
9	S_1 closed: WT ₁ FEC connected to the ac network
10 – 11	U_0 increased from 0 to 0.9 pu: WT ₁ energises the offshore ac network, establishing its voltage and frequency; all auxiliary power is provided from shore
15	$S_{a,k}$ closed: auxiliary loads energised
Sequence 2: Wind Power Takes Over	
20	Enough aerodynamic power available from the wind; WTs ready to produce power
20.1	FEC PLL and frequency and reactive power controls enabled for WTs 2–50; FEC active power proportional control enabled for WTs 2–50
20.5	S_2 closed: WT ₂ FEC connected to the ac network
21	WT ₁ FEC PLL and frequency and reactive power controls enabled; connected WT FECs regulate ac network voltage magnitude and frequency, while sharing the reactive power consumption/production
21.5 – 25.5	S_k closed at 0.5 s intervals for WTs 3–50: FECs from WTs 3–50 connected to the ac network
26	WT ₁ FEC active power proportional control enabled; connected FECs share the active power production
26.5	S_1 open: WT ₁ FEC disconnected from the ac network; all auxiliary power is provided from the wind
27	S_{WT} and $S_{dc,1}$ open: dc auxiliary supply disconnected; WT ₁ BEC takes over control of E_1
27.5	S_1 closed: WT ₁ FEC reconnected to the ac network

3.1. SEQUENCE 1: ENERGISATION FROM SHORE

At $t = 0$ s, the dc disconnectors S_{WT} and $S_{dc,1}$ are closed, so that the dc auxiliary supply effectively connects the dc bus bar of WT₁ to the HVdc link, $E_1 \approx E_R$. Between $t = 1$ s and $t = 6.39$ s, the onshore terminal energises the HVdc link and the dc bus bar of WT₁ as the direct voltage set point, E_R^* , is increased from 0 to the WT dc bus bar nominal voltage (approximately 5.39 kV), as illustrated in (a).

WT₁ main ac circuit breaker, S_1 , is closed at $t = 9$ s, and the corresponding FEC then energises the offshore ac network, establishing its voltage and frequency, as the offshore ac network voltage set point, U_0 , is increased from 0 to 0.9 pu between $t = 10$ s and $t = 11$ s, as shown in (d) and (e). In doing so, it draws about 339 kW from the onshore terminal, as illustrated in (c), to supply the no-load losses. The onshore terminal controller calculates the voltage drop in the HVdc link using the measured I_{dc} and estimated HVdc link resistance, \tilde{R}_{dc} , and compensates for it by increasing E_1 accordingly, maintaining E_R close to its reference value, as shown in (a) and (b). Inrush currents are avoided by energising all WT transformers at the same time with the voltage ramp. If, however, a WT is disconnected and needs to be re-energised by the established offshore ac network, proven solutions such as pre-insertion resistors and point on wave switching can be employed to reduce such currents.

At $t = 15$ s, ac circuit breakers $S_{a,k}$ are closed, and the auxiliary loads are energised, as depicted most notably in (c) and (g). As portrayed in (f), less than half of the WT nominal rms current is needed to energise the studied OWF with the proposed method. Furthermore, it requires an HVdc link current of less than 170 A, i.e. less than 10 % of its nominal current, as shown in (b), leaving enough HVdc link current capacity to energise the other two 400 MW OWFs in the same way. In the studied system, such current constitutes the necessary capacity of the dc auxiliary supply cables, introduced in the proposed energisation method. Such capacity can in turn determine the current limit for the corresponding protections.

3.2. SEQUENCE 2: WIND POWER TAKES OVER

Once enough aerodynamic power becomes available from the wind and WTs are ready to produce power, the regulators in the FEC PLL and frequency and reactive power control loops are enabled at $t = 20.1$ s for WTs 2–50, as are also the proportional terms of the regulators in the corresponding active power control loops. The main



ac circuit breaker of WT₂, S₂ is then closed at $t = 20.5$ s, so that the FEC from WT₂ is connected to the offshore ac network, as illustrated by (f). At $t = 21$ s, the regulators in the FEC PLL and frequency and reactive power control loops are enabled for WT₁, so that all connected WT FECs contribute autonomously to regulating the offshore ac network voltage magnitude and frequency, while sharing the reactive power consumption/production, as portrayed in (d), (e) and (h). The main ac circuit breakers, S_k, are then closed at 0.5 s intervals for the remaining WTs 3–50, between $t = 21.5$ s and $t = 25.5$ s, so that the corresponding WT FECs are connected to the offshore ac network, as depicted in (f) and (h). Each WT FEC synchronises automatically with the offshore ac network as it is connected.

At $t = 26$ s, the proportional term of the regulator in the WT₁ FEC active power control loop is enabled, so that all connected WT FECs share the active power production, as shown in (g). The WT₁ FEC is then disconnected from the offshore ac network at $t = 26.5$ s by opening S₁, as illustrated most notably by (f) and (g). From this moment forth, all auxiliary power is provided from the wind.

The dc auxiliary supply is disconnected at $t = 27$ s by opening S_{WT} and S_{dc,1}, as portrayed in (b), and the back-end converter (BEC) of WT1 takes over the control of the WT dc bus bar voltage, E1. At $t = 27.5$ s, the WT₁ FEC is reconnected to the offshore ac network by closing S₁, as depicted most notably by (f) and (g).

3.3. FURTHER COMMENTS

The proposed energisation method relies on accurate and independent control of the reduced voltage in the dc transmission network. This may require the use of, for example, a full-bridge modular multilevel converter and an additional set of measurement devices onshore. Likewise, additional protections (settings) may be required. Even though reliability requirements may not allow OWFs to do without local auxiliary energy sources, the method can certainly help reduce the reliance on such energy sources. Moreover, the applicability of the method to WTs with LV power converters will depend on the amount of auxiliary power to be transmitted through the HVdc cables and the thermal limits of such cables. Further research is needed to assess the applicability of the proposed energisation method and of DR connection technology in general to multiterminal HVdc networks.

4 CONCLUSIONS

The simulation results indicate that the proposed method is a suitable alternative for energising OWFs connected to HVdc via DRs. Using MV WT converters, the necessary auxiliary power can be provided to the studied OWF through the dc bus bar of the *energising* WT, while leaving enough HVdc link current capacity to energise the other OWFs in the same way. The method provides a robust and reliable alternative with minimal additional hardware: short dc cables connecting the dc bus bar of the energising WT to the HVdc link, and dc disconnectors at the terminals of such cables and at the DR dc terminals. This can be easily extended to more WTs in the OWF, increasing reliability by providing redundancy.

Once enough aerodynamic power becomes available from the wind and WTs are ready to produce power, wind power can take over the provision of the auxiliary power, and the dc auxiliary supply can be disconnected. With the considered grid-forming WT FEC controls, each FEC synchronises automatically with the offshore ac network as it is connected, and all connected FECs contribute autonomously to regulating the offshore ac network voltage magnitude and frequency, while sharing the active power production and the reactive power consumption/production.

5 ACKNOWLEDGEMENT

The authors gratefully acknowledge the contributions of Ömer Göksu and Lorenzo Zeni to the discussions leading up to this work. This work has received funding from the European Union's Horizon 2020 research and innovation programme under grant agreement No 691714.



REFERENCES

- [1] CIGRÉ Working Group B3.36, “Special Considerations for AC Collector Systems and Substations Associated with HVDC-Connected Wind Power Plants,” Paris, France, 2015.
- [2] R. M. Blasco-Giménez, S. C. Añó-Villalba, J. Rodríguez-D’Derlée, F. Morant-Anglada and S. I. Bernal-Pérez, “Distributed Voltage and Frequency Control of Offshore Wind Farms Connected With a Diode-Based HVdc Link,” *IEEE Transactions on Power Electronics*, vol. 25, no. 12, pp. 3095-3105, December 2010.
- [3] R. M. Blasco-Giménez, S. C. Añó-Villalba, J. Rodríguez-D’Derlée, S. I. Bernal-Pérez and F. Morant-Anglada, “Diode-Based HVdc Link for the Connection of Large Offshore Wind Farms,” *IEEE Transactions on Energy Conversion*, vol. 26, no. 2, pp. 615-626, March 2011.
- [4] E. V. Larsen, “Electric power transmission system for wind turbine and wind turbine farm and method for operating same”. United States Patent US 2011/0140511, 16 June 2011.
- [5] S. I. Bernal-Pérez, S. C. Añó-Villalba, R. M. Blasco-Giménez and J. Rodríguez-D’Derlée, “Efficiency and Fault Ride-Through Performance of a Diode-Rectifier- and VSC-Inverter-Based HVDC Link for Offshore Wind Farms,” *IEEE Transactions on Industrial Electronics*, vol. 60, no. 6, pp. 2401-2409, June 2013.
- [6] H. J. Knaak, P. Menke, T. Schröck, R. Schuster and T. Westerweller, “Wind farm connection having a diode rectifier”. International Patent WO 2014/131454 A1, September 2014.
- [7] T. Christ, S. Seman and R. Zurowski, “Investigation of DC Converter Nonlinear Interaction with Offshore Wind Power Park System,” in *Proceedings of the 2015 EWEA Offshore Conference*, Copenhagen, Denmark, 2015.
- [8] P. Menke, R. Zurowski, T. Christ, S. Seman, G. Giering, T. Hammer, W. Zink, F. Hacker, D. Imamovic, J. Thisted, P. Brogan and N. Goldenbaum, “2nd Generation DC Grid Access for Large Scale Offshore Wind Farms,” in *Proceedings of the 14th Wind Integration Workshop*, Brussels, Belgium, 2015.
- [9] J. Dorn, D. Ergin, T. Hammer, J. Knaak, P. Menke, J. Möller, R. Schuster, H. Stiesdal and J. Thisted, “Converter station with diode rectifier”. United States Patent US 2016/0013653 A1, 14 January 2016.
- [10] C. Prignitz, H. G. Eckel, S. Achenbach, F. Augsburg and A. Schön, “FixReF: A control strategy for offshore wind farms with different wind turbine types and diode rectifier HVDC transmission,” in *Proceedings of the IEEE 7th International Symposium on Power Electronics for Distributed Generation Systems (PEDG 2016)*, Vancouver, BC, Canada, 2016.
- [11] PROMOTioN, “Deliverable 3.1: Detailed functional requirements to WPPs,” 2016.
- [12] PROMOTioN, “Deliverable 3.2: Specifications of the control strategies and the simulation test cases,” 2017.
- [13] C. Neumann, H. G. Eckel, S. Achenbach and F. Augsburg, “Auxiliary Power Supply in a FixReF Controlled Offshore Wind Power Plant with Diode Rectifier HVDC Transmission,” in *Proceedings of the 16th Wind Integration Workshop*, Berlin, Germany, 2017.
- [14] PROMOTioN, “Deliverable 3.4: Results on control strategies of WPPs connected to DR-HVDC,” 2018.
- [15] L. Yu, R. Li and L. Xu, “Distributed PLL-Based Control of Offshore Wind Turbines Connected With Diode-Rectifier-Based HVDC Systems,” *IEEE Transactions on Power Delivery*, vol. 33, no. 3, pp. 1328-1336, June 2018.
- [16] R. Ramachandran, S. Poullain, A. Benchaib, S. Bacha and B. Francois, “AC Grid Forming by Coordinated Control of Offshore Wind Farm connected to Diode Rectifier based HVDC Link – Review and Assessment of Solutions,” in *Proceedings of the 20th European Conference on Power Electronics and Applications (EPE 2018 – ECCE Europe)*, Riga, Latvia, 2018.
- [17] I. Arana-Aristi, A. Hernández, G. H. Thumm and J. Holbøll, “Energization of Wind turbine Transformers With an Auxiliary Generator in a Large Offshore Wind Farm During Islanded Operation,” *IEEE Transactions on Power Delivery*, vol. 26, no. 4, pp. 2792-2800, October 2011.
- [18] J. Berggren, “Study of auxiliary power systems for offshore wind turbines: An extended analysis of a diesel gen-set solution,” Uppsala University, Uppsala, Sweden, 2013.
- [19] L. Cai, U. Karaagac and J. Mahseredjian, “Simulation of Startup Sequence of an Offshore Wind Farm With MMC-HVDC Grid Connection,” *IEEE Transactions on Power Delivery*, vol. 32, no. 2, pp. 638-646, April 2017.
- [20] O. Saborio-Romano, A. Bidadfar, J. N. Sakamuri, Ö. Göksu and N. A. Cutululis, “Novel Energisation Method for Offshore Wind Farms Connected to HVdc via Diode Rectifiers,” in *Proceedings of the 45th IEEE IES Annual Conference (IECON 2019)*, Lisbon, Portugal, 2019.